Imidazole-phosphate polymers : Acid-base properties, association with oligonucleotides and oligosilicates

Annenkov, Vadim V.

2021-05-01

Annenkov , V V , Aseyev , V , Zelinskiy , S N & Danilovtseva , E N 2021 , ' Imidazole-phosphate polymers : Acid-base properties, association with oligonucleotides and oligosilicates ' , Journal of Molecular Liquids , vol. 329 , 115598 . https://doi.org/10.1016/j.molliq.2021.115598

http://hdl.handle.net/10138/354285
https://doi.org/10.1016/j.molliq.2021.115598

Imidazole-phosphate polymers: acid-base properties, association with oligonucleotides and oligosilicates

Vadim V. Annenkov[a,*], Vladimir Aseyev[b], Stanislav N. Zelinskiy [a], Elena N. Danilovtseva [a]

[a]Limnological Institute Siberian Branch of Russian Academy of Sciences, Irkutsk, Russia

[b]Department of Chemistry University of Helsinki, Helsinki, Finland

[*]Corresponding author.

E-mail address: annenkov@lin.irk.ru; annenkov@yahoo.com (V. Annenkov)

Abstract

Water-soluble imidazole-phosphate copolymers were obtained by copolymerization of 1-vinylimidazole with vinyl acetate with subsequent phosphorylation under the action of phosphoric acid. The introduction of phosphate units into the vinylimidazole chain unexpectedly increased the basic properties of the polymer, the buffer capacity at pH 5-7 and activity in coordination with DNA oligonucleotides, which is important in gene therapy and genetic engineering. The condensation of silicic acid in the presence of new polymers leads to the appearance of composite nanoparticles, which are a model of silicon transport vesicles in nature, as well as a new precursor of silicon materials.

Keywords: 1-vinylimidazole; phosphate; oligonucleotides; siliceous nanoparticles; buffer capacity

Introduction

Polymeric water-soluble ampholites are an interesting class of macromolecules capable of changing the chain conformation, total charge and activity in coordination reactions depending on pH, ionic strength and other factors. Most of these polymers are based on amine and carboxylic groups, as the corresponding monomers are widely distributed. Imidazole cycles show properties of very weak base [1], and introduction of these

fragments into polymers allows increasing the buffer capacity of macromolecules [2]. Phosphate groups are found in some biopolymers, including DNA, RNA, silafins and silicidins [3,4]. Composites containing phosphoric acid or its derivatives and imidazole polymers are intensively studied as proton conducting membranes for fuel cells [5]. The ability of the imidazole cycle to form hydrogen and ionic bonds is crucial for high proton conductivity [6,7]. Synthetic polymers with phosphate moieties are not as common as carboxylic polymers. 2-Metacryloxyethylphosphate (MOEP) is a commercial monomer that allows introducing phosphate groups into polymers by radical copolymerization. Unfortunately, this substance contains an admixture of bifunctional monomer obtained by disproportionation of MOEP during storage of monomer [8]. This admixture gives rise to insoluble cross-linked products in copolymerization with 4-vinylimidazole [9]. Purification of the phosphate monomer does not solve the problem because in case of polymerization at an elevated temperature the disproportionation may occur [10]. Phosphorylation under the action of phosphoric acid allows the modification of polymers containing hydroxyl groups or vinyl acetate residues that are hydrolyzed during the reaction [11].

In this work we prepared imidazole-phosphate polymers by phosphorylation of 1-vinylimidazole (VI) and vinyl acetate (VA) copolymers. Acid-base properties of new polymers in aqueous media have been studied and their activity in interaction with polymeric acids with respect to DNA oligonucleotides and oligosilicates obtained by condensation of silicic acid has been investigated. Water-soluble polymers containing electron-donor groups are able to interact with primary silica particles, which are formed from silicic acid. This reaction was found more than hundred years ago [12-14] and is well reviewed [15-18]. This century study of silicic acid condensation in the presence of polymers had gained an impetus from discovery of silaffins [19] -

polyamine and phosphate modified proteins from siliceous frustules of diatom algae. The attempts to simulate formation of biogenic silica resulted in finding polymers capable to give stable dispersions (colloidal solutions) of composite nanoparticles during $Si(OH)_4$ condensation in the presence of polymer [20-26]. These nanoparticles are promising agents for drug delivery including transfection agents in gene therapy [10,20,25-35]. Stable dispersions of polymer-silica nanoparticles are a new biomimetic precursor of siliceous materials that can be obtained by interaction with opposite charged particles [20,26] and by applying a 3D printer [36].

Experimental

Reagents

Vinyl acetate (VA), 1-vinylimidazole (VI), n-hexane, dimethylformamide (DMF), azobisisobutyronitrile (AIBN), 4-(methylamino)phenol hemisulfate salt (metol), $Na_2HPO_4 \cdot 12H_2O$, $Na_2SiO_3*5H_2O$, ammonium molybdate tetrahydrate, 0.1 M HCl, NaCl, phosphoric acid (85 wt. % in H_2O) were of reagent grade (Merck, Fisher, or Acros Chemicals). Deuterium oxide (D_2O, 99.8 atom D%) was purchased from Sigma-Aldrich. DMF was dried with anhydrous $CuSO_4$ and 3Å molecular sieves, followed by distillation. AIBN was recrystallized from ethanol. VA and VI were distilled prior use under atmospheric and reduced pressure, respectively. FAM 3'-tagged DNA oligonucleotide was purchased from Evrogen JSC, Russia and applied as 10 μM solution. 21-mer FAM-DNA sequence was GATCTCATCAGGGTACTCCTT.

Synthesis of Polymers

1-vinylimidazole - vinylacetate copolymerization

VI and VA were copolymerized in DMF (2.5 mL DMF *per* 5 g of monomers) with 1% (from the monomers mass) of AIBN as initiator, in argon atmosphere at 60 ^{o}C for 24 h.

The initial molar monomer ratio (VI: VA) was 30: 70 and 60: 40 for VI-P-53-6 and VI-P-69-10 samples respectively. Copolymers were precipitated into hexane and vacuum dried, yield was 60% (VI-P-53-6) and 74% (VI-P-69-10).

Phosphorylation of 1-vinylimidazole - vinylacetate copolymers

A vigorously stirred mixture of 2.36 g of a VI-VA copolymer with 236 g of 43% (w/w) phosphoric acid aqueous solution was heated from 30 °C up to 100 °C for about 60 min. Then stirring was kept on at 100 °C for 100 min followed by cooling with a cold water bath to room temperature. After that the resulted reaction mixture was dialyzed against distilled water during 24 h, against saturated solution of NaCl during 24 h, and anew against distilled water during three days. Thermo Scientific SnakeSkin Dialysis Tubing (3.5K MWCO, 22 mm) was applied for the dialysis. The dialysis residue was concentrated with a rotary evaporator, filtered through a 0.2 µm membrane and freeze-dried to yield 1.45 g of VI-P-53-6. VI-P-69-10 was prepared analogically with the same acid solution / copolymer mass ratio, yield was 2.34 g from 3.58 g of the initial VI-VA copolymer.

Copolymer characterization

NMR and FT-IR spectroscopy

^{31}P and ^{13}C NMR spectra were recorded on a DPX 400 Bruker instrument in D_2O at 160 MHz for ^{31}P and 100 MHz for ^{13}C NMR. Relaxation delays (D1) between pulses in ^{13}C NMR were set at 10 s, which allowed to prevent the impact of relaxation effects on the integral intensity of ^{13}C NMR peaks (according to preliminary experiments). This is more than five times more than the relaxation times in acrylic polymers [37]. IR spectra were recorded with an Infralum FT-801 spectrometer using KBr pellets.

Molar mass of the copolymers

Light scattering experiments were conducted with a Brookhaven Instruments BI-200SM goniometer, a BI-TurboCorr digital crosscorrelator, and a BI-CrossCorr dual detector consisting of two BI-DS1 detectors. A Sapphire 488-100 CDRH laser from Coherent GmbH operating at the wavelength of λ_o=488 nm (vertically polarized) and the power adjusted to 50 mW was a light source in dynamic LS. Molar mass was measured using a diode laser Mini-L30 (λ_o=637.6 nm; 30 mW; Brookhaven Instruments). The intensities measured in counts of photons per second, cps, were normalized with respect to the Rayleigh ratio of toluene. The temperature of the samples was controlled by means of a Lauda RC 6C thermostat. The increment of refractive index, dn/dc, was measured using an Optilab rEX refractometer from Wyatt Technology operated at λ_o=632.8 nm. All the measurements were performed at 20ºC.

Copolymers were dissolved in 0.1M HCl with addition of 0.1M NaCl. This solvent destroyed aggregates of copolymer macromolecules and solution showed monomodal size distribution according to DLS data. Results of molar mass measurement are presented in Table 1.

Table 1 Composition and molar mass of the copolymers

Copolymer	Composition, mol% of units			dn/dc,	M_w, Da	R_g,	A_2,
	VI	~OPO_3H_2	~OH	$mL \cdot g^{-1}$		nm	$cm^3 \cdot mol \cdot g^{-2}$
VI-P-53-6	53	6	41	0.1709	51,000	17	1.2
VI-P-69-10	69	10	31	0.1923	91,000	26	1.3

Study of acid-base properties of the copolymers and their interaction with oligonucleotides and oligosilicates

Light scattering experiments

Zeta-potential (ζ) and hydrodynamic radius (R_h) were measured at 20 °C with a Zetasizer Nano-ZS ZEN3600 (Malvern Instruments Ltd., UK) operated at 173° scattering angle and at the wavelength of 633 nm. These device was applied to measure kinetics of silicic acid condensation in the presence of copolymers, ζ and R_h of copolymer-DNA complexes.

The Brookhaven Instruments device (described above) was applied to measure dynamic and static light scattering at 30-150° angles with 15° step in the case of stable products of silicic acid condensation in the presence of copolymers. R_h and R_g were obtained from these multiangle experiments. Certain assumptions are unavoidable for the studied system. Thus, the measured values of the diffusion coefficients are apparent, not absolute and ideally should be determined at infinite dilution, which is not possible in this case. The size of the aggregates is not big enough in comparison to the wavelength to apply special fitting functions such as Berry, Debye, or Guinier plots, or the functions for specific geometries (i.e., rod, solid sphere, etc.). Therefore, we used the initial slope of the Zimm function within its limit of $qR_g<1.2$ for all studied particles. Yet, even for the solution of VI-P-69-10 at pH 10, the Zimm function is linear below $qR_g=3.3$ within the experimental error, which is demonstrated with corresponding Fig. S1 in the Supplementary Material. Our third assumption is that the composite polymer-silica nanoparticles have uniform and rather homogeneous distribution of all components within the particles. Organic polymer and silica have different refractive indexes and, which in the case of inhomogeneous distribution of material may affect measured value of R_g. However, we found no evidences of such inhomogeneity. SLS experiments for R_g

determination were performed only on those systems, which show monomodal size distributions between 30° and 150° scattering angle. In such cases, relaxation rates (Γ) of corresponding correlation functions of electric field $g_1(t)$ show linear dependence of q^2. This is an additional evidence of the monomodal (moderately polydispersed) distributions and translational self-diffusion of the studied particles.

Potentiometry measurements

Potentiometry experiments were performed with a "Multitest" ionometer (JSC Semico, Novosibirsk, Russian Federation) applying combined pH-electrode at 20 ± 0.02 °C. Potentiometric titration of aqueous solutions of copolymers was carried out with a solution containing 10-11 mM of imidazole units, pH was brought up to 2.5 by 0.1 M HCl and solution was titrated with 0.1 M NaOH solution. Buffer capacity was calculated from the potentiometry data according to the International Union of Pure and Applied Chemistry (IUPAC) recommendations as a derivative of the added NaOH concentration versus pH (the number of moles of strong base required to change the pH by one unit when added to one liter of the solution) [38].

Silicification experiments

Silicification experiments were started from copolymer solutions adjusted to pH 11 with 0.1 M NaOH, after that sodium silicate was added. The obtained solutions were titrated with 0.1 M HCl. Experiments on silicic acid condensation at pH 5.5, 7 and 10 were performed starting from the same solutions and the desired pH was adjusted with 1 M HCl over 30-60 s on the basis of predetermined volumes of the acid.

Concentration of orthosilicic acid (monomer and dimer) was estimated by the molybdenum blue colorimetric method [15,39]. This method is based on the formation of a silicic acid molybdate complex followed by reduction with ‘metol’ and

measurement by colorimetry at 810 nm. The selected reaction conditions allow only interaction of monomers and dimers of silicic acid with a molybdate reagent without hydrolysis of more condensed species. Kinetic data on silicic acid condensation were processed using a plot of $1/[Si(OH)_4]^2$ versus time, which gives a straight line for the first 60 min of reaction [20].

Composite siliceous precipitates obtained at pH 7 were collected by centrifugation (3000 g, 5 min), twice washed with cold water (2-4 °C), and freeze-dried. Scanning electron microscopy (SEM) and energy dispersive X-ray analysis (EDAX) were performed using FEI Quanta 200 instruments. The samples were placed on double-sided sticky carbon tape mounted on aluminum sample holders and then sputter-coated with gold using a SDC 004 (BALZERS) device. The coating settings (working distance 50 mm, current 15 mA, time 75 s) correspond to 12 nm gold coating according to the device manual.

Study of the copolymer - DNA interaction by gel electrophoresis

The interaction between DNA oligonucleotides and polymers was investigated by electrophoresis on agarose gel. Electrophoresis experiments were performed with a Mini-Sub (7 × 10 cm) Cell GT System (Bio-Rad Laboratories, Inc.), an ELF-4 power supply (DNA-Technology LLC) and a TCP-20LC transilluminator (Vilber Lourmat), operated at 254 nm. Complexes were prepared by mixing solutions of the polymer and oligonucleotides in 40 mM Tris acetate buffer (pH 7.2). 10 μM oligonucleotide solutions and 4 or 10 mM copolymer solutions (calculating on VI units) were applied as stock solutions. The solutions were mixed according to desired N: P value (imidazole-nucleotide ratio) and were diluted with the buffer to 2.5 μM oligonucleotides concentration. The samples were incubated at room temperature for 30 min and placed into the wells of the 1% agarose gel. Free oligonucleotide, as a control, was also loaded

onto the gel. The gel running buffer was 40 mM Tris acetate (adjusted to pH 7.2) and 1 mM EDTA. A glycerol gel loading buffer was used (0.5% sodium dodecyl sulfate, 0.1 M EDTA (pH = 8), and 50% glycerol for 10× reagent). The gel was run at 90 V for 25 min and the fluorophore-tagged oligonucleotide was visualized on a UV transilluminator.

Results and discussion

Copolymer synthesis and characterization

Imidazole-phosphate polymers were obtained from VI-VA copolymers by phosphorylation with phosphoric acid (Fig. 1). Initial VI-VA copolymers are statistic copolymers: the monomers reactivity ratios are 1.5 and 0.2 for VI and VA, respectively [40]. The average length of the monomeric blocks (Table S1 in the Supplementary Material) was calculated according to [41] and the values obtained (1-3 units) confirm the statistical distribution of the monomer units. Products after phosphorylation were purified with dialysis and freeze-dried. IR spectra (Fig. 2) contain bands attributed to imidazole and protonated imidazole cycles [42]: 3100 cm^{-1} (ν CH, ring), 2300-2900 cm^{-1} (broad band, ν NH, protonated ring), 1577 and 1544 cm^{-1} (ν C-C and C-N, protonated ring), 1500 cm^{-1} (ν C-C and C-N, ring), 1420 cm^{-1} (ν ring), 1290 cm^{-1} (δ CH and ν C-N, ring), 1090 cm^{-1} (δ CH and ν, ring), 825 cm^{-1} (γ CH and γ ring) and 662 cm^{-1} (ν N-C and δ ring). VA units reveal themselves as 1090 cm^{-1} (ν CO) band which is more broad and intensive comparing with imidazole band. Intensive ester bands (1735 cm^{-1}, ν C=O and 1235 cm^{-1}, ν CO) present in spectrum of initial VI-VAc copolymer but disappear after hydrolysis. A weak band at 970 cm^{-1} is possibly arisen from phosphate units (ν COP).

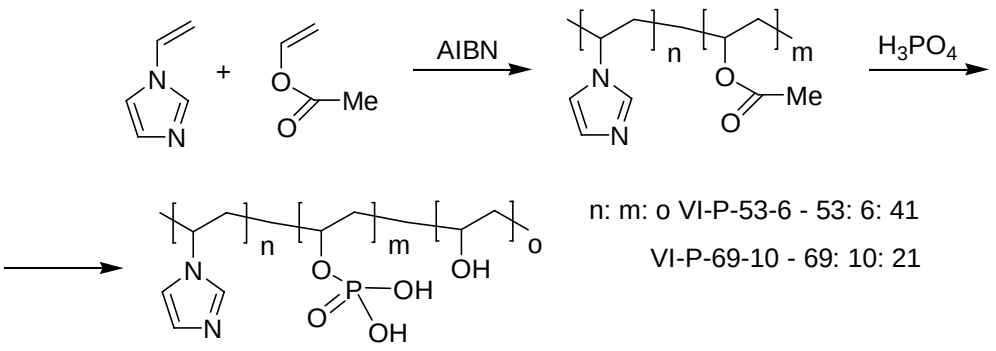

Fig. 1. Synthesis of imidazole-phosphate polymers.

^{31}P NMR spectra of VI-P-53-6 and VI-P-69-10 copolymers (Fig. 3(a)) contain a signal at 3.4-3.5 ppm which agree with data of phosphoric acid monoesters [43]. Phosphoric acid and Na_2HPO_4 of the same concentration (ca. 50 mg/mL) show signal at 0.05-0.06 ppm and this signal was not observed in spectra of copolymers. ^{13}C NMR spectra of the copolymers (Fig. 3(b)) contain the following signals: 116-137 ppm (imidazole cycle), 61-67 ppm (**C**H-OH in hydrolyzed VA units), 51-57 ppm (**C**H-N in VI units) and 37-45 ppm (**C**H_2 groups of the main chain). Phosphorylated VA units give a weak signal from **C**H-OP carbon atom which was not appropriate for quantitative analysis. Non-hydrolyzed VA units were expected as signals near 21 ppm (**C**H_3) and 170 ppm (**C**=O). The absence of these signals confirms complete hydrolysis of VA units.

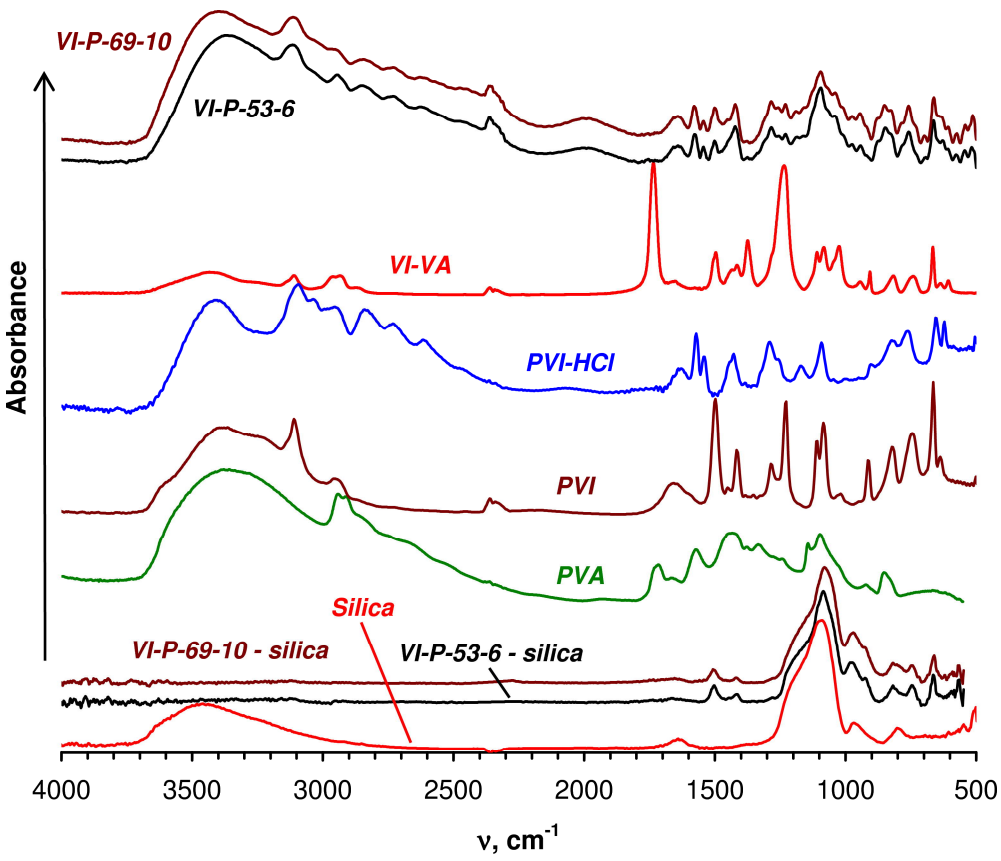

Fig. 2. IR spectra of imidazole-phosphate polymers VI-P-53-6 and VI-P-69-10, VI-VA copolymer (precursor of VI-P-53-6), PVI and PVI hydrochloride, poly (vinyl alcohol), siliceous composites prepared by $Si(OH)_4$ condensation in the presence of new copolymers at pH 7 and silica obtained from sodium silicate (100 mM aqueous solution) acidified with HCl to pH 7.

Composition of the copolymers was estimated by an analysis for phosphorus [11] and ^{13}C NMR data for imidazole cycles (116-137 ppm) and CH-OH in hydrolyzed VA units (61-67 ppm). VI-P-53-6 and VI-P-69-10 samples contain 53 and 69 mol.% of VI units, 6 and 10 mol.% of phosphorylated VA units respectively.

According to static light scattering (Table 1) molar mass of the copolymers is 51 and 91 kDa for VI-P-53-6 and VI-P-69-10 respectively.

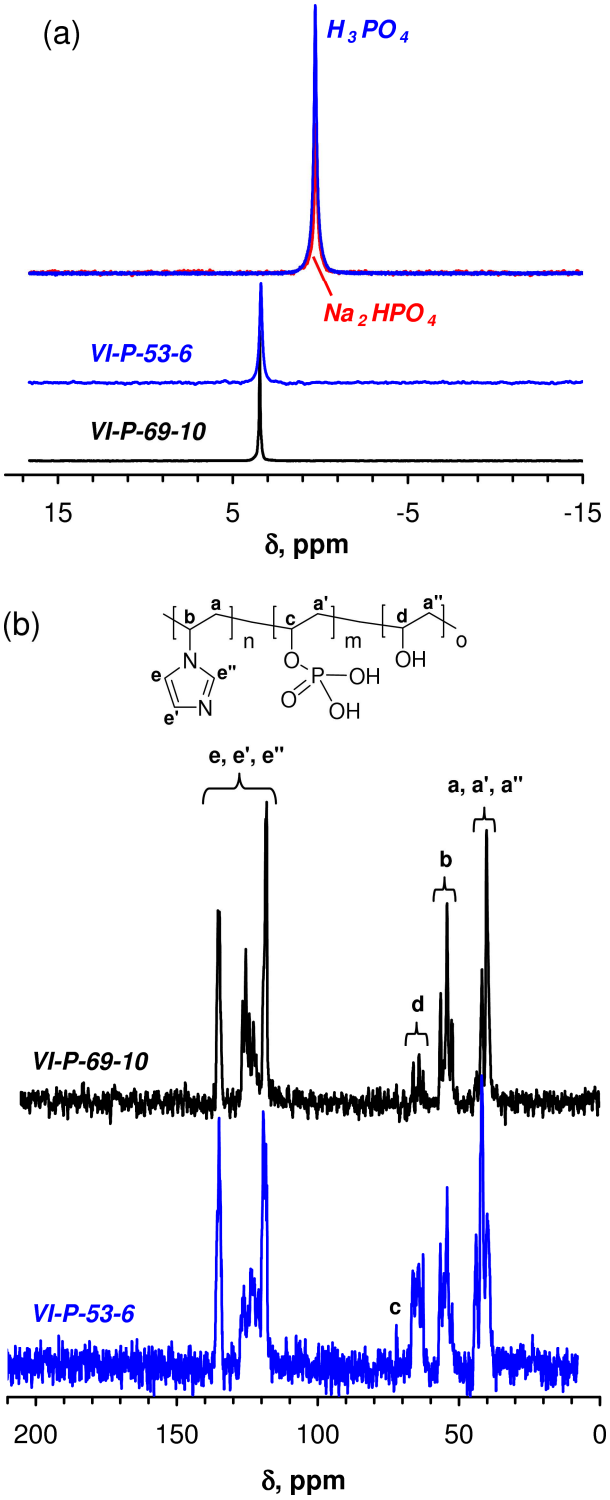

Fig. 3. ^{31}P (a) and ^{13}C (b) NMR spectra of the copolymers

Acid-base properties of the copolymers in aqueous solution

Aqueous polymer solutions have pH values of 5.2-5.5 and were titrated with 0.1 M NaOH after adding 0.1 M HCl to pH 2.5 (Fig. 4). VI-P-53-6 copolymer precipitated at

pH 7.5-9.5 (Table 2). Titration curves of the copolymers show one distinct inflection at pH 9-9.5 similar to PVI. Phosphoric acid in concentration comparable to concentration of polymeric phosphate groups shows two inflections: in acidic area corresponding to neutralization of the first ~P-OH group and second group is neutralized at pH 9.3 which agree with theoretical titration curve. According to [44] first and second ionization constants of monoalkyl esters of phosphoric acid are close to values of H_3PO_4 but the inflection in acidic area was not observed for copolymers nor for model PVI-H_3PO_4 mixture. Probably, imidazole links work as a buffer to suppress a sharp increase in pH in the acidic area. In general, the titration curves of the copolymers lie above the curve of the model mixture PVI-H_3PO_4, indicating a higher basicity of the copolymers.

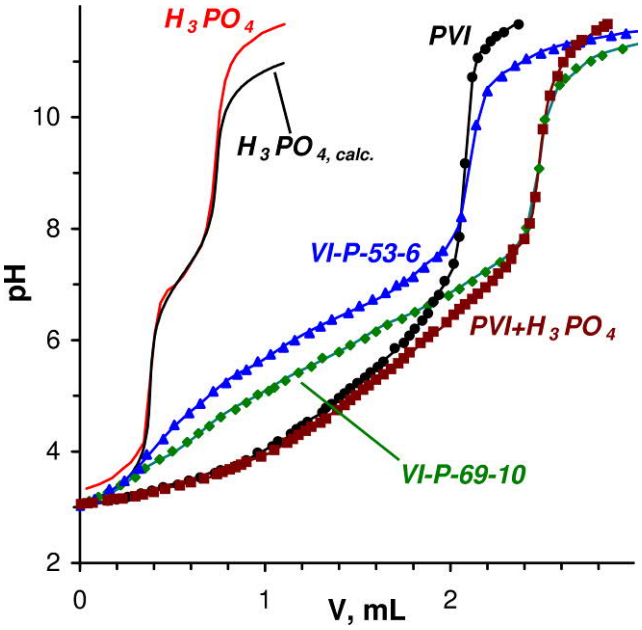

Fig. 4. Potentiometry titration data for copolymers, PVI, phosphoric acid and PVI - phosphoric acid mixture. PVI and copolymer concentration correspond to 10 mM of imidazole units, phosphoric acid – 1.5 mM. Solution volume – 20 mM, titrant – 0.1 M NaOH. Theoretical curve for phosphoric acid (H_3PO_4, calc) was obtained from dissociation constants (pK_a) = 2.14, 7.20 and 12.37 [45].

Table 2 Heterogeneity intervals for polymers and polymer-sodium silicate mixtures (potentiometry titration data)

System	Heterogeneity interval, pH
VI-P-53-6	7.5-9.5
VI-P-69-10	-
VI-P-53-6 + Na_2SiO_3	5.8-7.0
VI-P-69-10 + Na_2SiO_3	5.7-8.1

Earlier [2], we found that the buffer capacity of PVI is higher than that of polymeric amines, e.g., polyethylenamine, in the acidic region. Buffer capacity of the new imidazole-phosphate copolymers is considerably higher than values of PVI or PVI-H_3PO_4 mixture at pH 5-7 (Fig. 5). The high buffer capacity of polymer amines is explained by the concept of "proton sponge" [46], which implies variability of pK amine groups attached to the polymer chain depending on pH and degree of neutralization. This factor exists for PVI and as mentioned above imidazole units are active in formation of hydrogen bonds. In the case of imidazole-phosphate copolymers we suppose formation of intra- and interchain hydrogen bonds involving phosphate units. The ability to form ~N-H^+···N~ bonds increases amount of protonable imidazole units and "proton sponge" activity (Fig. 6). The presence of associated imidazole units explains domination of protonated cycles in the IR spectra of the copolymers (Fig. 2) in spite of low amount of acidic phosphate units (6-10 comparing with 53-56 mol% of VI units). Hydrogen bonds in imidazole – phosphate systems are treated is an important part of proton conductivity [7]. The increase in the buffer capacity of new copolymers indicates the prospects of using phosphate-containing polymers as carriers for the delivery of genes capable of leaving the endosome to cytoplasm [46].

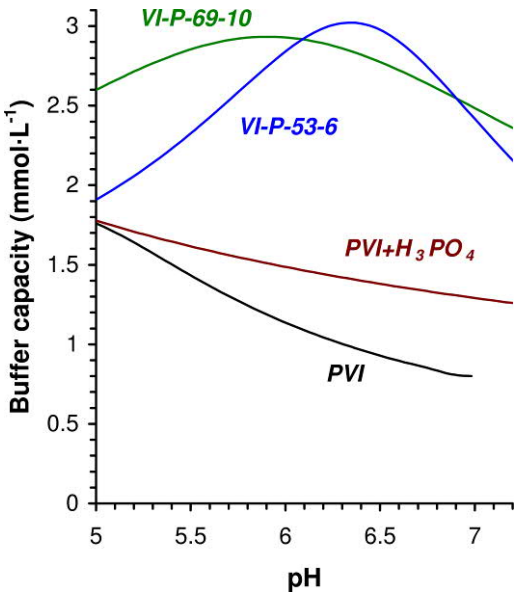

Fig. 5. Dependence of buffer capacity on pH.

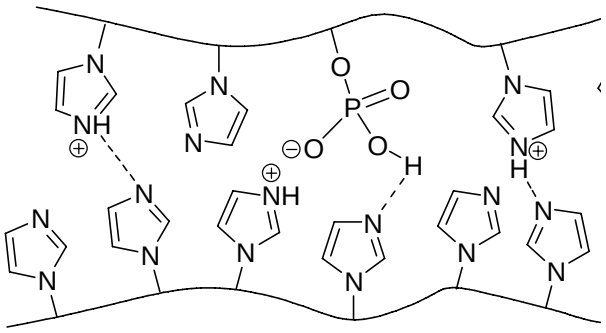

Fig. 6. Hydrogen and ionic bonds in the imidazole-phosphate copolymers.

Complexation of the new copolymers with oligonucleotides

The ability of new copolymers to interact with DNA oligonucleotides was studied with electrophoresis (Fig. 7). Full DNA involvement in the complex was observed at N:P 40 and 140 ratios for VI-P-53-6 and VI-P-69-10, respectively. These values are considerably lower than that for PVI (N:P = 2000) [2]. This is quite unexpected, because before our work the only way to increase PVI activity when interacting with nucleic acids was to introduce amine or quaternary nitrogen fragments into the polymer [2, 47-50]. In any case, imidazole groups are present in the complex to a large extent more than DNA units, in fact, one macromolecule of the copolymer contains no more

than one DNA molecule. We suppose this DNA molecule is involved into associated structures of the copolymer similar to shown in Fig. 6. The average number of imidazole and phosphate units in the VI-P-53-6 copolymer is 360 and 40, respectively (based on the molar mass and composition, Table 1). Similar values for VI-P-69-10 are 725 and 105, which provides a sufficient number of free imidazole units for complexation with 21-mer DNA.

The DLS data (Fig. 8(a)) show a bimodal particle size distribution in the case of free copolymers, while the addition of a small amount of oligonucleotide results in monomodal distributed particles with a diameter of 120-200 nm. This result can be interpreted as the involvement of oligonucleotide molecules and free copolymer macromolecules in associates that are additionally stabilized by interactions between nucleotides and imidazole units. Similar multi-molecular complexes DNA-polymer complexes were discussed recently [51,52]. The ζ-potential of free copolymers is +5-10 mV (Fig. 8(b,c)) and association with DNA does not change this value significantly. The particle size and positive charge of copolymer complexes with DNA are sufficient for penetration into living cells [53].

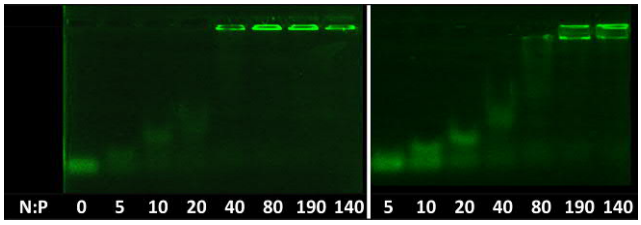

Fig. 7. Gel electrophoresis data for VI-P-53-6 (left) and VI-P-69-10 (right) complexes with 21-mer FAM-DNA at pH 7.2. DNA concentration in the polymer-oligonucleotide mixture was 2.5 μM. N: P values correspond to imidazole-nucleotide ratios.

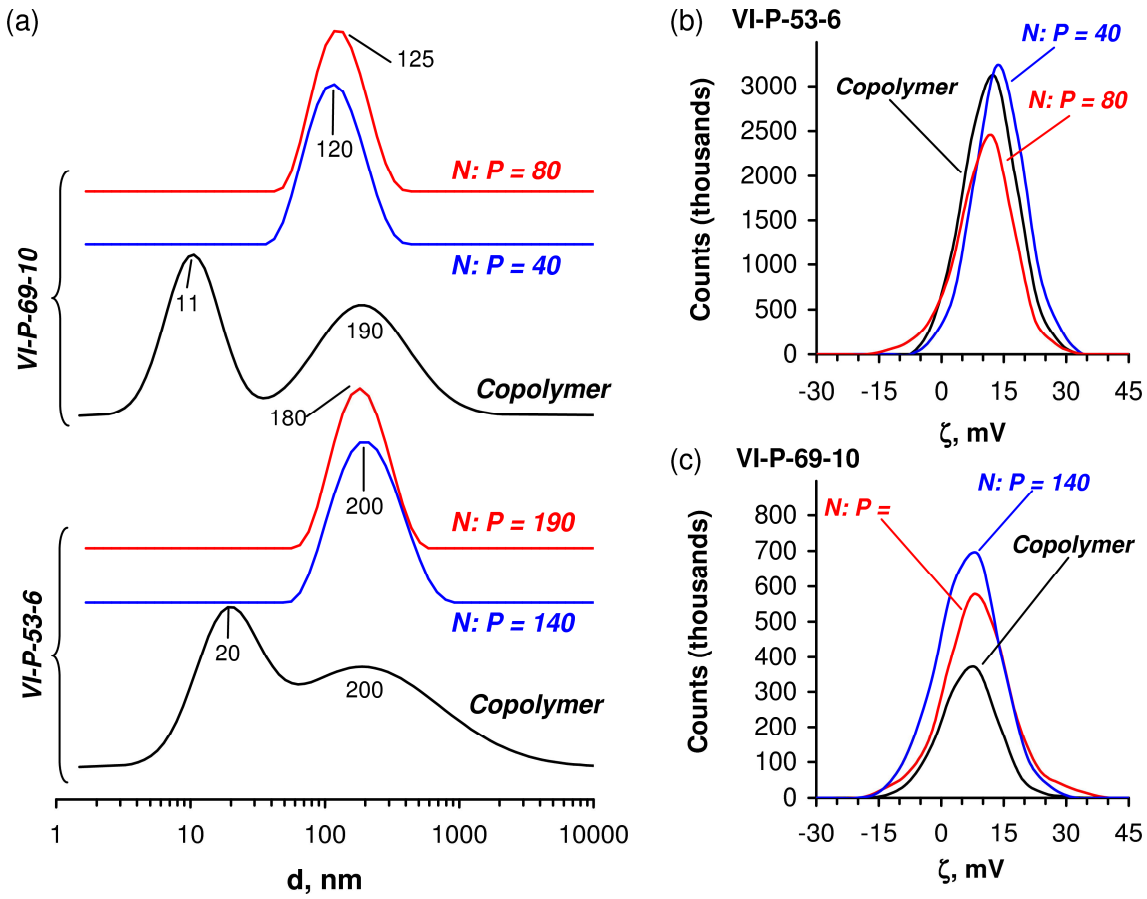

Fig. 8. Size distribution (a) and ζ-potential (b,c) of the particles in copolymer solution at pH 7.2 and of the copolymer - oligonucleotide complexes. Copolymer concentration was 0.5 mg/mL, N: P values correspond to imidazole-nucleotide ratios in the complexes. The data were obtained with Zetasizer Nano-ZS instrument.

Influence of the copolymers on silicic acid condensation

Condensation of silicic acid in the presence of new imidazole-phosphate copolymers was studied in solutions containing 10 mM Na_2SiO_3 and the same concentration of imidazole units of the copolymers. Preliminary titration data (Table 2) showed precipitation at neutral pH values and reaction in the solution was studied at pH 5.5 and 10. pH 5.5 corresponds to pH in silica deposition vesicles (SDV) of diatoms [54] and pH 10 is in the beginning of pH range of active $Si(OH)_4$ condensation [15].

The rate of condensation of silicic acid in the presence of copolymers was estimated by colorimetric molybdenum blue method [15] (example data are shown in Fig. 9). The

both copolymers increase initial condensation rate, especially VI-P-69-10. This polymer slightly inhibit condensation after several hours of the reaction. Previous data [27,23] revealed a decrease in the rate of condensation with PVI at any stage of the reaction due to stabilization of low-active non-ionized siliceous particles in contrast to more basic polymeric amines [20]. We assume that primary siliceous particles are involved in the more basic structures responsible for the high buffer capacity, which increases the ionization of silanol groups and the condensation rate. A large number of condensed silica particles are present after several hours of reaction, these particles interact with copolymers, like ordinary PVI - silica hydrogen bonds, which can slightly inhibit the reaction.

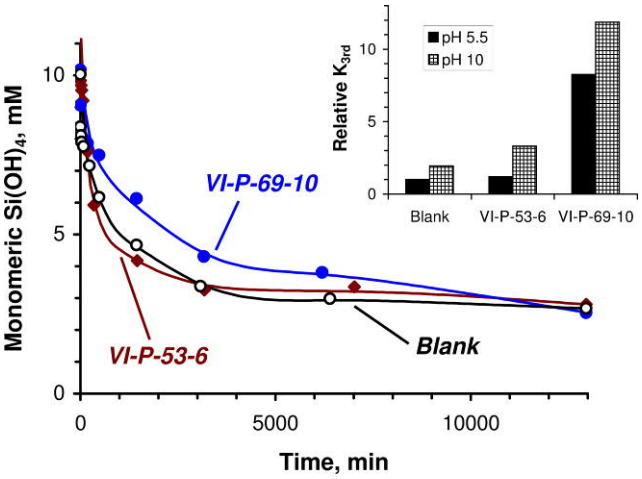

Fig. 9. Example data set showing the effect of the polymers on condensation of silicic acid at pH 5.5 and the k_{third} for the $Si(OH)_4$ at pH 5.5 and 10. All rate constants are relative to the blank at pH 5.5. Initial solutions contained 10 mM of $Si(OH)_4$ and copolymers in concentration corresponded to 10 mM of imidazole units.

Copolymers in aqueous medium exist as a mixture of 7-15 nm and 75-200 nm particles according to DLS data (Fig. 10). These small particle sizes can be attributed to individual macromolecules and the larger particles are evidently associates. Condensation of silicic acid in the presence of copolymers is accompanied by

redistribution of particle sizes, which results in monomodal distribution of sizes in VI-P-69-10 system (Fig. 10). These colloidal systems are stable for more than three weeks. A similar effect was observed for other polymer systems - $Si(OH)_4$ [20,23] and was explained by the formation of composite polymer-silica nanoparticles. The solutions that showed monomodal size distribution were studied with multiangle light scattering, which gives more reliable results. Combination of DLS and SLS data (Table 3) allowed us to obtain R_g and R_h values which ratio R_g/R_h gives information about particle nature [55]. The data of pure siliceous nanoparticles (0.6-0.8) are close to microgels (0.3-0.6) and homogeneous (hard) spheres (0.778). Composite nanoparticles formed at pH 10 (R_g/R_h = 1.15) are similar to dense objects (dendrimers, star structures at Θ-conditions). Particle size considerably decrease at pH 5.5 and R_g/R_h = 0.63 is typical for microgels. ζ potential for the composite nanoparticles was -18±1 and +45±2 mV at pH 10 and 5.5 respectively. These data are consistent with an increase in the hydrogen bonding abilities between the imidazole and ~Si-OH groups at pH 5.5 due to the neutralization of ~Si-ONa groups. Size of the composite nanoparticles obtained at pH 5.5 is close to electron dense vesicles in diatoms which were hypothesized as silicon transport vesicles [56].

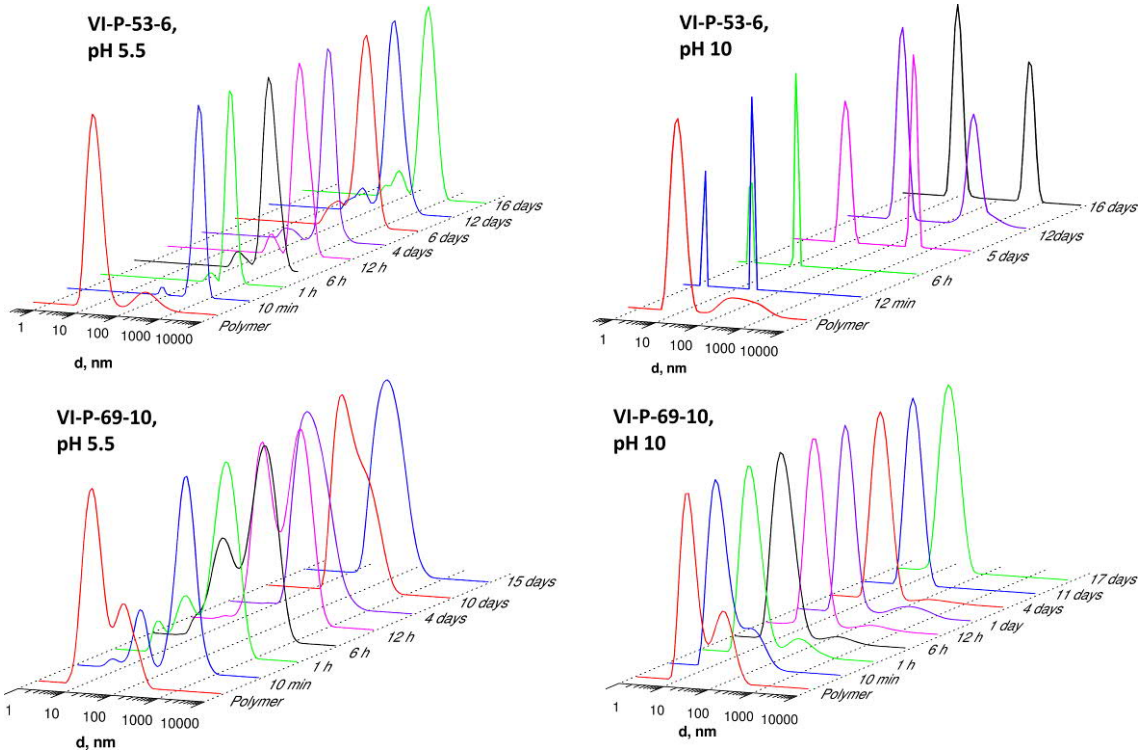

Fig. 10. Size distribution of the particles formed on condensation of silicic acid in the presence of imidazole-phosphate polymers at pH 5.5 and 10. The data were obtained with Zetasizer Nano-ZS instrument.

Composite precipitates obtained at pH 7 were studied using scanning electron microscopy (SEM, Fig. 11). Both copolymers produce a sediment built from nanoparticles, which are close to the size of the DLS data. The nanoparticles are sticked together to spheres from 500 nm to several μm in diameter. VI-P-69-10 gives more smoothed particles comparing with VI-P-53-6. The precipitates contain silicon and phosphorus from copolymer according to EDAX data (Fig. 11, g-i). IR spectra of the composites (Fig. 2) show presence of siliceous structures: bands at 1082 (with a shoulder at 1200 cm1) and 810 cm^{-1} correspond to SiO stretching motions, and vibrations of the SiOH bond are observed at 970 cm^{-1} [57]. Bands at 1500, 1415, 745 and 660 cm^{-1} are arisen from the copolymers.

Table 3 Multiangle DLS and SLS data of composite nanoparticles

System	R_g, nm	R_h, nm	R_g/R_h
Na_2SiO_3, pH 10	6.2	9.7	0.64
Na_2SiO_3, pH 5.5	10.9	13.2	0.83
VI-P-69-10 + Na_2SiO_3, pH 10	99.8	86.4	1.15
VI-P-69-10 + Na_2SiO_3, pH 5.5	28.8	45.8	0.63

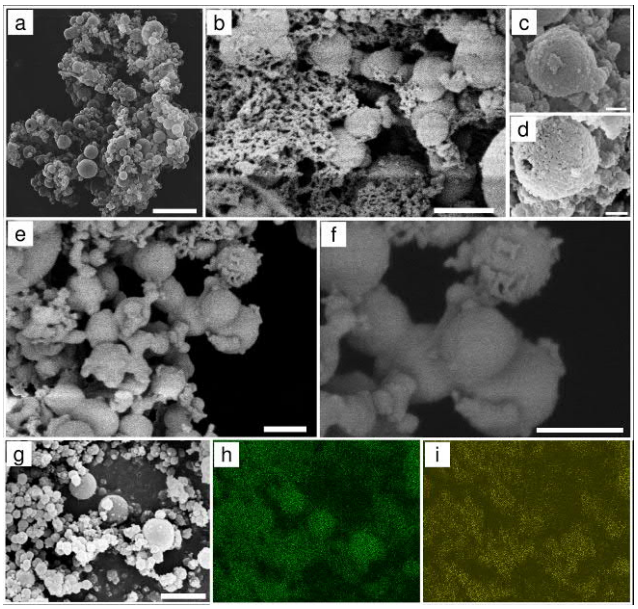

Fig. 11. SEM images of composite precipitates (VI-P-53-6 (a-d) and VI-P-69-10 (e-g)) obtained at pH 7 and EDAX silicon (h) and phosphorus (i) mapping of the precipitate VI-P-69-10. Scale bar 0.5 μm (b-f) and 5 μm (a and g-i).

Conclusions

We have obtained new imidazole-phosphate polymers by phosphorylation of 1-vinylimidazole - vinyl acetate copolymers. These copolymers showed a higher buffer capacity at pH 5-7 compared to PVI or polyethyleneimine. This phenomenon was

explained by the association between imidazole and phosphate units, which increase the overall basicity of the polymer due to facilitating hydrogen bonding between protonated and free imidazole cycles. The copolymers are active in coordination with DNA oligonucleotides, and the imidazole-to-DNA ratio at full DNA binding is an order of magnitude lower than the value for PVI. Copolymer-oligonucleotide complexes are monomodally distributed particles with a diameter of 120-200 nm, which is sufficient for penetration into living cells. These results show that new imidazole-phosphate copolymers are promising structures in the design of nucleic acid delivery systems in gene therapy and genetic engineering. Condensation of silicic acid is accelerated in the presence of new copolymers and it results in the formation of stable dispersion of composite nanoparticles at pH 5.5 and 10, while at pH 7 precipitates in the form of spheres with diameters ranging from 500 nm to several μm were obtained. Size of the composite nanoparticles obtained at pH 5.5 (R_h = 45.8, R_g = 28.8 nm) is close to electron dense vesicles in diatom algae which were hypothesized as silicon transport vesicles.

Acknowledgments

This work was supported by the Russian Academy of Sciences under Grant # AAAA-A19-119100490016-4); the Russian Foundation for Basic Research under Grant # 19-04-00926. The authors wish to thank the Center of Ultramicroanalysis (Limnological Institute) and Baikal Nanotechnology Center (Irkutsk National Research Technical University) for providing equipment and the Irkutsk Supercomputer Center of SB RAS for providing the access to HPC-cluster "Akademik V.M. Matrosov". The extremely constructive suggestions of the anonymous referee enabled us to improve the manuscript considerably.

References

[1] N.L. Mazyar, V.V. Annenkov, V.A. Kruglova, S.M. Anan'ev, E.N. Danilovtseva, A.V. Rokhin, S.V. Zinchenko, Acid-base properties of poly(1-vinylazoles) in aqueous solution, Russ. Chem. Bull. 45 (2000) 2013-2017. https://doi.org/10.1023/A:1009571908805.

[2] E.N. Danilovtseva, S.N. Zelinskiy, V.A. Pal'shin, G. Kandasamy, U.M. Krishnan, V.V. Annenkov, Poly(1-vinylimidazole) prospects in gene delivery, Chinese J. Polym. Sci. 37 (2019) 637–645. https://doi.org/10.1007/s10118-019-2240-1.

[3] S. Wenzl, R. Hett, P. Richthammer, M. Sumper, Silacidins: highly acidic phosphopeptides from diatom shells assist in silica precipitation in vitro, Angew. Chem. Int. Ed. 47 (2008) 1729-1732. https://doi.org/10.1002/anie.200704994.

[4] N. Kroger, S. Lorenz, E. Brunner, M. Sumper, Self-assembly of highly phosphorylated silaffins and their function in biosilica morphogenesis, Science 298 (2002) 584-586. https://doi.org/10.1126/science.1076221.

[5] S.U. Celik, A. Bozkurt, S.S. Hosseini, Alternatives toward proton conductive anhydrous membranes for fuel cells: heterocyclic protogenic solvents comprising polymer electrolytes, Prog. Polym. Sci. 37 (2012) 1265-1291. https://doi.org/10.1016/j.progpolymsci.2011.11.006.

[6] G.F. Mangiatordi, V. Butera, N. Russo, D. Laage, C. Adamo, Charge transport in poly-imidazole membranes: a fresh appraisal of the Grotthuss mechanism, Phys. Chem. Chem. Phys. 14 (2012) 10910-10918. https://doi.org/10.1039/c2cp23727j.

[7] Y. Hori, T. Suetake, Y. Shiota, K. Yoshizawa, Y. Shigeta, T. Ida, M. Mizuno, Local structures and dynamics of imidazole molecules in poly(vinylphosphonic acid)−imidazole composite investigated by molecular dynamics, ACS Appl. Polym. Mat. 2 (2020) 1561-1568. https://doi.org/10.1021/acsapm.9b01222.

[8] L. Grondahl, S. Suzuki, E. Wentrup-Byrne, Influence of a diene impurity on the molecular structure of phosphate-containing polymers with medical applications, Chem. Commun. 28 (2008) 3314-3316. https://doi.org/10.1039/b803223h.

[9] A. Bozkurt, B. Karadedeli, Copolymers of 4(5)-vinylimidazole and ethyleneglycol methacrylate phosphate: synthesis and proton conductivity properties, React.

Funct. Polym. 67 (2007) 348–354. https://doi.org/10.1016/j.reactfunctpolym.2007.01.010.

[10] V.V. Annenkov, V.A. Pal'shin, E.N. Danilovtseva, Water-soluble copolymers of 2-methacryloyloxyethyl phosphate: synthesis and properties, e-Polymers (2012) no. 024. https://doi.org/10.1515/epoly.2012.12.1.244.

[11] M. Banks, J.R. Ebdon, M. Johnson, Influence of covalently bound phosphorus-containing groups on the flammability of poly(vinyl alcohol), poly(ethylene-co-vinyl alcohol) and low-density polyethylene, Polymer 34 (1993) 4547-4556. https://doi.org/10.1016/0032-3861(93)90163-5.

[12] Th. Craham, XXXV.-On liquid diffusion applied to analysis, J. Chem. Soc. 15 (1862) 216-270. https://doi.org/10.1039/JS8621500216.

[13] F. Mylius, E. Groschuff, α- und β-kieselsäure in lösung, Ber. Dtsch. Chem. Ges. 39 (1906) 116-125. https://doi.org/10.1002/cber.19060390124.

[14] W.J. Lesley, Studies on reactions between hydrophilic sols. (Part II.), Trans. Faraday Soc. 26 (1930) 69-78. https://doi.org/10.1039/TF9302600069.

[15] R. Iler, The Chemistry of Silica, Wiley, New York, 1982.

[16] J. Brinker, G.W. Scherer, Sol-Gel Science: the Physics and Chemistry of Sol-Gel Processing, Academic Press, London, 1990.

[17] A.D. Pomogailo, Metallopolymer Nanocomposite-Macromulecular Metallocomplexes as Precursors for Polymers, Polymer Inorganics, and Bionanocomposites, in A.S Abd-El-Aziz, C.E. Carraher, C.U. Pittman, J. Zeldin. (Eds), Macromolecules containing metal and metal-like elements, Wiley and Sons Inc., New York, 2005, pp. 87-220. https://doi.org/10.1002/0471773263.ch4

[18] V.V., Annenkov, E.N. Danilovtseva, V.A. Pal'shin, O.N. Verkhozina, S.N. Zelinskiy, and U.M. Krishnan, Silicic acid condensation under the influence of water-soluble polymers: from biology to new materials, RSC Adv. 7 (2017) 20995-21027. https://doi.org/10.1039/c7ra01310h.

[19] N. Kroger, R. Deutzmann, M. Sumper, Polycationic peptides from diatom biosilica that direct silica nanosphere formation, Science 286 (1999) 1129-1132. https://doi.org/10.1126/science.286.5442.1129.

[20] V.V. Annenkov, E.N. Danilovtseva, V.A. Pal'shin, V.O. Aseyev, A.K. Petrov, A.S. Kozlov, SV. Patwardhan, C. Perry, Poly(vinyl amine)-silica composite nanoparticles: models of the silicic add cytoplasmic pool and as a silica

precursor for composite materials formation, Biomacromolecules 12 (2011) 1772-1780. https://doi.org/10.1021/bm2001457.

[21] E. Brunner, L. Lutz, M. Sumper, Biomimetic synthesis of silica nanospheres depends on the aggregation and phase separation of polyamines in aqueous solution, Phys. Chem. Chem. Phys. 6 (2004) 854–857. https://doi.org/10.1039/b313261g.

[22] V.V. Annenkov, E.N. Danilovtseva, E.A. Filina, Y.V. Likhoshway, Interaction of silicic acid with poly(1-vinylimidazole), J. Polym. Sci., Part A: Polym. Chem. 44 (2006) 820–827. https://doi.org/10.1002/pola.21190.

[23] E.N. Danilovtseva, V.A. Pal'shin, Y.V. Likhoshway, V.V. Annenkov, Condensation of silicic acid in the presence of co(1-vinylimidazole–acrylic acid), Adv. Sci. Lett. 4 (2011) 616–621. https://doi.org/10.1166/asl.2011.1262.

[24] N. Gouda, K. Miyata, R.J. Christie, T. Suma, A. Kishimura, S. Fukushima, T. Nomoto, X.Y. Liu, N. Nishiyama, K. Kataoka, Silica nanogelling of environment-responsive PEGylated polyplexes for enhanced stability and intracellular delivery of siRNA, Biomaterials 34 (2013) 562–570. https://doi.org/10.1016/j.biomaterials.2012.09.077.

[25] V.V. Annenkov, V.A. Pal'shin, O.N. Verkhozina, L.I. Larina, E.N. Danilovtseva, Composite nanoparticles: a new way to siliceous materials and a model of biosilica synthesis, Mater. Chem. Phys. 165 (2015) 227–234. https://doi.org/10.1016/j.matchemphys.2015.09.022.

[26] M. Sumper, Biomimetic patterning of silica by long - chain polyamines, Angew. Chem., Int. Ed. 43 (2004) 2251–2254. https://doi.org/10.1002/anie.200453804.

[27] V.V. Annenkov, E.N. Danilovtseva, Y.V. Likhoshway, S.V. Patwardhan, C. Perry, Controlled stabilisation of silicic acid below pH 9 using poly(1-vinylimidazole), J. Mater. Chem. 18 (2008) 553-559. https://doi.org/10.1039/b716367n.

[28] M.A. Grachev, V.V. Annenkov, Y.V. Likhoshway, Silicon nanotechnologies of pigmented heterokonts, BioEssays 30 (2008) 328–337. https://doi.org/10.1002/bies.20731.

[29] D. Belton, S.V. Patwardhan, V.V. Annenkov, E.N. Danilovtseva, C.C. Perry, From biosilicification to novel materials: optimizing hydrophobic domains and resistance to protonation of polyamines, Proc. Natl. Acad. Sci., U. S. A. 105 (2008) 5963-5968. https://doi.org/10.1073/pnas.0710809105.

[30] V.V., Annenkov, S.V. Patwardhan, D. Belton, E.N. Danilovtseva, C.C. Perry, A new stepwise synthesis of a family of propylamines derived from diatom silaffins and their activity in silicification, Chem. Commun. 14 (2006) 1521–1523. https://doi.org/10.1039/b515967a.

[31] E.N. Danilovtseva, V.V. Annenkov, E.A. Shmeleva, L.V. Serd'uk, S.I. Leshuk, Synthetic water-soluble polymers in self-organizing nanosystems for immynology, Proceeding of the IASTED International Conference on Nanotechnology and Applications, Crete, Greece, 2008. pp. 27-32.

[32] M. Liang, S. Patwardhan, E. Danilovtseva, V. Annenkov, C. Perry, Imidazole catalysed silica synthesis:progress towards understanding the role of histidine in (bio)silicification, J. Mater. Res. 24 (2009) 1700-1708. https://doi.org/10.1557/jmr.2009.0223.

[33] E. Danilovtseva, V. Aseyev, M. Karesoja, V. Annenkov, Sorption of silicic acid from non-saturated aqueous solution by a complex of zinc ions with poly(vinylamine), Eur. Polym. J. 45 (2009) 1391-1396. https://doi.org/10.1016/j.eurpolymj.2009.01.002.

[34] P. Overton, E. Danilovtseva, E. Karjalainen, M. Karesoja, V. Annenkov, H. Tenhu, V. Aseyev, Water-dispersible silica-polyelectrolyte nanocomposites prepared via acid-triggered polycondensation of silicic acid and directed by polycations, Polymers 8 (2016) 96. https://doi.org/10.3390/polym8030096.

[35] E.N. Danilovtseva, V. Aseyev, O.Yu. Belozerova, S.N. Zelinskiy, V.V. Annenkov, Bioinspired thermo- and pH-responsive polymeric amines: multimolecular aggregates in aqueous media and matrices for silica/polymer nanocomposites, J. Colloid Interface Sci. 446 (2015) 1-10. https://doi.org/10.1016/j.jcis.2015.01.021.

[36] S.H. Yangand, I.S. Choi, Bio‐inspired silicification on patterned surfaces generated by microcontact printing and layer‐by‐layer self‐assembly, Chem.–Asian J. 4 (2009) 382–385. https://doi.org/10.1002/asia.200800381.

[37] S. Yamazaki, I. Noda, A. Tsutsumi, l3C NMR relaxation of poly(acrylic acid) in aqueous solution. Effects ofcharge density on local chain dynamics, Polym. J. 32 (2000) 87–89. https://doi.org/10.1295/polymj.32.87.

[38] E.B. Sandeli, T.S. West, Recommended nomenclature for titrimetric analysis, Pure Appl. Chem. 18 (1969) 427−436. https://doi.org/10.1351/pac196918030427.

[39] D. Belton, G. Paine, S.V. Patwardhan, C.C. Perry, Towards an understanding of (bio)silicification: the role of amino acids and lysine oligomers in silicification, J. Mater. Chem. 14 (2004) 2231-2241. https://doi.org/10.1039/b401882f.

[40] K.L. Petrak, Reactivity of some vinylimidazoles towards other vinyl monomers in radical copolymerization, J. Polym. Sci.: Polym. Lett. Ed. 16 (1978) 393–399. https://doi:10.1002/pol.1978.130160802

[41] E.N. Zilberman, Parameters of microstructure of multicomponent copolymers, Vysokomol. Soed. Ser. B 21 (1979) 33-36.

[42] J.L. Lippert, J.A. Robertson, J.R. Havens, J.S. Tan, Structural studies of poly(N-vinylimidazole) complexes by infrared and Raman spectroscopy, Macromolecules 18 (1985) 63-67. https://doi.org/10.1021/ma00143a010.

[43] L.D. Quin, A.J. Williams, Practical Interpretation of P-31 NMR Spectra and Computer-Assisted Structure Verification. Advanced Chemistry Development Inc., Toronto, 2004.

[44] W.D. Kumler, J.J. Eiler, The acid strength of mono and diesters of phosphoric acid. the n-alkyl esters from methyl to butyl, the esters of biological importance, and the natural guanidine phosphoric acids, J. Am. Chem. Soc. 65 (1943) 2355–2361. https://doi.org/10.1021/ja01252a028.

[45] K.J. Powell, P.L. Brown, R.H. Byrne, T. Gajda, G. Hefter, S. Sjöberg, H. Wanner, Chemical speciation of environmentally significant heavy metals with inorganic ligands. Part 1: The Hg^{2+}, Cl^{-}, OH^{-}, CO_3^{2-}, SO_4^{2-}, and PO_4^{3-} aqueous systems (IUPAC Technical Report), Pure Appl. Chem. 77 (2005) 739-800. https://doi.org/10.1351/pac200577040739.

[46] O. Boussif, F. Lezoualc'h, M.A. Zanta, M.D. Mergny, D.A. Scherman, B. Demeneix, J.P. Behr, A versatile vectorfor gene and oligonucleotide transfer into cells in culture and invivo: polyethylenimine, Proc. Natl. Acad. Sci. U. S. A. 92 (1995) 7297−7301. https://doi.org/10.1073/pnas.92.16.7297.

[47] Y. Hori, T. Suetake, Y. Shiota, K. Yoshizawa, Y. Shigeta, T. Ida, M. Mizuno, Local structures and dynamics of imidazole molecules in poly(vinylphosphonic acid)−imidazole composite investigated by molecular dynamics, ACS Appl. Polym. Mat. 2 (2020) 1561-1568. https://doi.org/10.1021/acsapm.9b01222.

[48] S. Asayama, T. Hakamatani, H. Kawakami, Synthesis and characterization of alkylated poly(1-vinylimidazole) to control the stability of its DNA polyion

complexes for gene delivery, Bioconjugate Chem. 21 (2010) 646–652. https://doi.org/10.1021/bc900411m.

[49] X.T. Shuai, T. Merdan, F. Unger, T. Kissel, Supramolecular gene delivery vectors showing enhanced transgene expression and good biocompatibility, Bioconjugate Chem. 16 (2005) 322-329. http://dx.doi.org/10.1021/bc0498471.

[50] C.W. Pouton, P. Lucas, B.J. Thomas, A.N. Uduehi, D.A. Milroy, S.H. Moss, Polycation-DNA complexes for gene delivery: a comparison of the biopharmaceutical properties of cationic polypeptides and cationic lipids, J. Control. Release 53 (1998) 289-299. http://dx.doi.org/10.1016/S0168-3659(98)00015-7.

[51] E. Haladjova, G. Mountrichas, S. Pispas, S. Rangelov, Determination of Intimate composition of theranostic polyplexes based on (co)polymers of poly(vinyl benzyl trimethylammonium chloride), Macromol. Chem. Phys. 219 (2018) 1700428. https://doi.org/10.1002/macp.201700428

[52] Y. Niebel, M.D. Buschmann, M. Lavertu, G. De Crescenzo, Combined analysis of polycation/ODN polyplexes by analytical ultracentrifugation and dynamic light scattering reveals their size, refractive index increment, stoichiometry, porosity, and molecular weight, Biomacromolecules 15 (2014) 940−947. https://doi.org/10.1021/bm4018148

[53] R. Wang, X. Wang, X. Jia, H. Wang, W. Li, J. Li, Impacts of particle size on the cytotoxicity, cellular internalization, pharmacokinetics and biodistribution of betulinic acid nanosuspensions in combined chemotherapy, Int. J. Pharm. 588 (2020) 119799. https://doi.org/10.1016/j.ijpharm.2020.119799

[54] E.G. Vrieling, W.W.C. Gieskes, T.P.M. Beelen, Silicon deposition in diatoms: control by the pH inside the silicon deposition vesicle, J. Phycol. 35 (2002) 548–559. http://dx.doi.org/10.1046/j.1529-8817.1999.3530548.x.

[55] W. Burchard, Solution Properties of Branched Macromolecules, in: J. Roovers (ed) Branched Polymers II. Advances in Polymer Science, v. 143. Springer, Berlin, Heidelberg, 1999, pp 113-194 |https://doi.org/10.1007/3-540-49780-3_3.

[56] A.M.M. Schmid, D. Schulz, Wall morphogenesis in diatoms:deposition of silica by cytoplasmic vesicles, Protoplasma 100 (1979) 267–288. http://dx.doi.org/10.1007/BF01279316.

[57] M.J. Adeogun, J.N. Hay, Structure control in sol-gel silica synthesis using ionene polymers. 2: Evidence from spectroscopic analysis, J. Sol-Gel Sci. Technol. 20 (2001) 119-128. http://dx.doi.org/10.1023/A:1008795321600.

Table S1. Average length of the monomeric blocks in VI-VA copolymers

Copolymer	L_1 (VI)	L_2 (VA)
VI-P-53-6	2.0	1.8
VI-P-69-10	2.6	1.2

Calculation of R_h and R_g from multiangle scattering

Certain assumptions are unavoidable for the studied system. Thus, the measured values of the diffusion coefficients are apparent, not absolute and ideally should be determined at infinite dilution, which is not possible in this case. The size of the aggregates is not big enough in comparison to the wavelength to apply special fitting functions such as Berry, Debye, or Guinier plots, or the functions for specific geometries (i.e., rod, solid sphere, etc.). Therefore, we used the initial slope of the Zimm function within its limit of qR_g<1.2 for all studied particles. Yet, even for the solution of VI-P-69-10 at pH 10, the Zimm function is linear below qR_g = 3.3 within the experimental error, which is demonstrated with corresponding Fig. S1. Our third assumption is that the composite polymer-silica nanoparticles have uniform and rather homogeneous distribution of all components within the particles. Organic polymer and silica have different refractive indexes and, which in the case of inhomogeneous distribution of material may affect measured value of Rg. However, we found no evidences of such inhomogeneity. SLS experiments for Rg determination were performed only on those solutions, which show monomodal size distributions between 30° and 150° scattering angle. In such solutions, relaxation rates (Γ) of corresponding correlation functions of electric field g1(t) show linear dependence of q^2. This is an additional evidence of the monomodal (moderately polydispersed) distributions and translational self-diffusion of the studied particles.

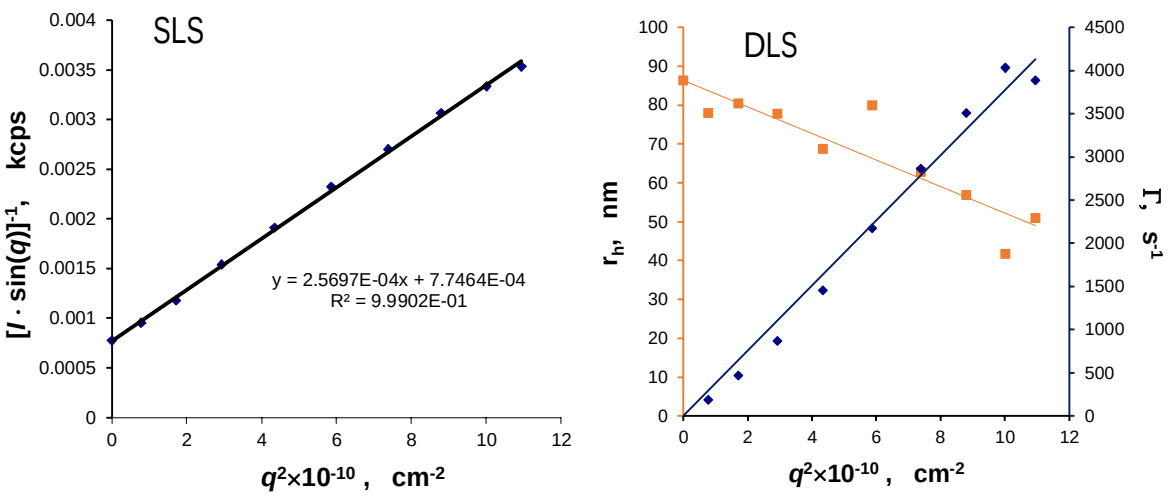

Fig. S1. SLS plot of the inverse excess intensity versus the square of the scattering angle. Corresponding r_g for VI-P-69-10 + Na2SiO3 at pH 10 is 99.8 nm. DLS plot shows the angular dependence of r_h (multi exponential fit, CONTIN) and the relaxation rates (Γ) of corresponding correlation functions of electric field $g_1(t)$. Γ was calculated using the second order cumulant fit.